RADIATION EFFECTS ON COMPOSITE STRUCTURES

FINAL REPORT
FOR
CONTRACT NAS3-21050

LOCKHEED-GEORGIA COMPANY

A DIVISION OF LOCKHEED AIRCRAFT CORPORATION

ER-10056

RADIATION EFFECTS ON COMPOSITE STRUCTURES

FINAL REPORT
FOR
CONTRACT NAS8-21050

January 1969

Prepared For:

GEORGE C. MARSHALL SPACE FLIGHT CENTER

Prepared By:

LOCKHEED GEORGIA NUCLEAR LABORATORY

LOCKHEED GEORGIA NUCLEAR LABORATORY
Lockheed-Georgia Company - A Division of Lockheed Aircraft Corporation

FOREWORD

This document constitutes the final report of work performed for the Marshall Space Flight Center under Contract NAS8-21050 by the Lockheed Georgia Nuclear Laboratory. The report describes the response of Pegasus micrometeorite panels and electronics to a simulated space electron environment.

TABLE OF CONTENTS

LIST OF FIGURES

ABSTRACT

The implementation and performance of a series of tests to determine the effects of a near space temperature and radiation environment on the Pegasus micrometeorite detection system is described. A discussion of detector panel response to induced charges is also presented. Analyses of test data indicates little degradation of system data due to environmental changes.

1.0 INTRODUCTION

In order to collect data concerning micrometeoroids, the National Aeronautics and Space Administration has deployed a group of earth orbiting satellites (Pegasus Project) utilizing the capacitor discharge technique to detect micrometeorite "hits." This velocity dependent discharge waveshape coupled with satellite orbital attitude information is used to determine particle size, velocity, and direction of travel. Close examination of the available Pegasus data revealed the possibility of not only "hits" being detected but also a spontaneous discharge phenomenon thought to be produced by electrons trapped and stored within the mylar dielectric of the detector panels. This theory was confirmed by LCNL personnel in an earlier test series utilizing a standard Pegasus panel subjected to a near space electron spectrum (Figure 1). It was the results of this investigation (documented in engineering report ER-8582, "Radiation Effects on Composite Structures," Contract NAS8-20206) which brought forth the many questions this second and third series of tests will endeavor to answer.

Section 3.0 covers the second series of tests and concerns the detector panels as a subsystem dealing primarily with the following:

(1) The effects of temperature and radiation cycling simulating the Pegasus environment.

(2) The effect of the foam separator material in the electron breakdown phenomenon.

(3) Buildup time from onset of radiation until breakdown pulses occur.

(4) The correlation, if any, between the pulse heights and breakdown areas by limiting the area of irradiation.

(5) A cursory investigation of the response of the Pegasus electronics and the effect of multi-breakdowns on the monitoring circuits. (This is covered more completely in Section 4.0).

In an effort to quantitatively determine the effects of space radiation on the Pegasus panel - electronics combination. A third test series described in Section 4.0 was proposed as a contract extension. These experiments were approved and later defined in a joint Lockheed-MSFC meeting.

The tests all utilized the Pegasus electronics and involved the following:

(1) Determination ot electron induced pulse rate as a function of temperature.

(2) Determination of pulse spectra during warm-up cycles.

(3) Pulse record during radiation cycling at a constant low temperature.

(4) Pulse record during simulated orbital radiation and temperature cycling.

2.0 SUMMARY OF RESULTS

The test specimens were standard 20" x 40" Pegasus panels having 25 mil mylar insulation and aluminum backings of 8 and 16 mil thickness. These panels were mounted within a temperature controlled portion of a large vacuum chamber (Figure 2). A remotely controlled 62 mil stainless steel electron shield was deployed between the panel and the source plaque enabling radiation cycling. The temperature of the entire assembly was varied and controlled from ambient to -62°C while subjected to an atmosphere of 10^{-6} torr.

The first series of test objectives were investigated simultaneously while others required special procedures. The results are listed in the order of questions presented in the introduction.

(1) The overall effects of temperature and radiation cycling simulating the Pegasus orbital environment were negligible. The panel could be "conditioned," however, to produce anomalies in pulse production. If, for instance, the panel were subject to prolonged radiation at a given temperature, subsequent radiation cycling would result in a decrease in pulse production and amplitude. Increasing the temperature of the panel after being radiated would increase pulse production and amplitude.

(2) All tests indicate the foam sandwich material can be disregarded as a contributor to pulse production.

(3) No correlation was found between time to pulse buildup and temperature in the -32°C to -62°C range. The process appeared to be random with the first pulse appearing from ten to thirty minutes after onset of irradiation. Discharge persisted for approximately seventeen hours after the radiation shield was introduced with the pulse rate and amplitude being

random in nature.

(4) The pulse output spectrum of four panel sections having different exposed cross sectional areas were compared. The spectrums were similar and indicate no connection between panel size and pulse occurrence or amplitude.

(4) As expected the Pegasus electronics was capable of verifying a radiation induced pulse. It is also capable of "seeing" the panel discharge caused by temperature changes. This phenomenon was investigated further and described more fully in the next test series.

Tests with the Pegasus electronics and panels yield the following conclusions:

(1) There is no specific temperature in the range of $0^{\circ}C$ to $-60^{\circ}C$ where an increase in detected pulses can be expected.

(2) Some low level pulses will be verified without giving an indication on the lighting circuits (power supply - panel identification).

(3) Pulse production caused by short term radiation exposure is not detected.

(4) Discharge pulses produced by some means other than temperature or nuclear radiation are detected with sufficient amplitude to trigger the indicator circuits.

(5) Since only one panel was connected in our experiments and multiple channel light indications were recorded it is assumed there must be some cross coupling within the electronics package (in some cases the correct channel would not be indicated but an erroneous one would).

(6) The channel light indications are accumulative in that if they are not reset additional lights will come on as large verified pulses occur.

It is felt that the normal Pegasus orbital temperature and radiation cycling cannot be considered a continual or predictable source of erroneous "hits." There appears to be a strong possibility, however, that some other phenomena such as electromagnetic or electrostatic discharge could be of concern. This and the actual operating characteristics of the electronics package warrant further investigation.

3.0 PANEL RESPONSE EXPERIMENTS

This series of tests was designed to provide additional information on the electrical response of the micrometeorite panel to an electron radiation exposure similar to that encountered in its normal earth orbit.

3.1 TEST DESCRIPTION

The panels to be evaluated were mounted in the temperature controlled vacuum chamber while connected, by special fittings and cable, to the external monitoring system depicted in Figure 5. A Lockheed designed pulse inverter and channel splitter was built to properly match the input of the spectrum analyzer.

The foam separator analysis was performed first, with the panel connected as in Figure 6. Two sixteen hour runs were made under each condition shown, the first enabling charges present in both the foam and mylar to be recorded and the second detecting the mylar breakdowns only. The panel temperature was maintained at $-62^{\circ}C$.

The buildup time measurement was taken next. The panel was cooled to $-50^{\circ}C$ in a 10^{-6} torr vacuum. As the electron shield was removed the panel temperature decreased further to $-62^{\circ}C$. Repeated runs were made under this configuration with the time span from the onset of radiation to the first pulse being recorded. This series was then rerun while the temperature was varied in steps between $-62^{\circ}C$ and $-32^{\circ}C$ to determine if any temperature dependence existed within this range. Before each test run the panel was heated to $23^{\circ}C$ to release any stored charges within the mylar.

The third experiment of this series was designed to determine the correlation, if any, between the maximum amplitude and the panel area exposed to radiation.

It had been found from previous observations that the panel as a whole does not break down, but highly localized areas of space charge are responsible for its output. The maximum amplitude pulse seen has been on the order of 2.5 to 3.0 volts. From this data and existing theory it was postulated that the largest radiated area required for breakdown analysis was in the range of 2.5 square centimeters.

To accomplish this task, a standard 20" x 40", 16 mil aluminum Pegasus panel was etched into four separate capacitors using a solution of sodium hydroxide to remove the aluminum from the mylar. Each of these capacitors represented essentially the same area as shown in Figure 3. An electron shield was then fabricated from 62 mil aluminum and divided into four quadrants, each representing the area over one of the four etched capacitors. Holes were drilled in each of the shields four quadrants limiting the area of panel exposure to 0.100, 0.242, 0.599, and 1.267 square centimeters (Figure 4). The shield was then mounted flush with the four section Pegasus panel. Individual coaxial cables were run from the four capacitors to the instrumentation area.

The chamber temperature was lowered to -62°C with each panel being monitored to obtain "individual" pulse height spectrums. Since the total capacitor area had been reduced it was necessary to extend the irradiation time to 72 hours.

The series of evaluations, that of radiation and temperature cycling, was carried out over an extended period of time employing increasing and decreasing temperatures and various panel conditioning techniques. The monitoring arrangement was, again, that of Figure 5.

The final data run involved the Pegasus micrometeorite detection system (Figure 7) and a 16 mil detector panel. This panel (at -62°C) was exposed to radiation for a period of several days. Four to six "hits" were observed over each 24-hour period. The radiation was then removed from the panel by imposing a shield between it and

the source. The system was again allowed to operate for several days during which no "hits" were observed. The panel was then exposed to radiation cycling for 10 minutes out of a 110 minute cycle.

No "hits" were observed, but, because this experiment could not be carried out properly, the results are not considered conclusive. The principle compromise was that the cycling could only be carried out during the working day resulting in relatively few cycles. Following this experiment, the radiation was stopped and the temperature control turned off allowing the panel to gradually warm up to room temperature. At some point during the warm-up cycle, a "hit" was observed. It was found in previous phases of the project that many low voltage pulses occurred when the panel was allowed to heat up following radiation exposure. Evidently one pulse was of sufficiently high voltage to "count" on the Pegasus electronics. The results of the test indicate that further work was required to quantitatively determine the effects of space radiation on the Pegasus electronics.

3.2 DISCUSSION OF PANEL RESPONSE

The formation of negative space charge regions in solid dielectrics during exposure to a flux of high energy electrons has been substantiated experimentally.[1-8] The theory of the trapping of injected electrons, and subsequent spontaneous release of trapped charge, in Mylar has been treated in the literature.[1-2] The observed phenomena cannot readily be interpreted in terms of macroscopic electrical properties such as volume resistivity or dielectric constant but would seem to be related to charge storage capacity associated with existing traps or radiation induced traps with sufficient density and at deep enough levels to permit regions of space charge to exist. The distribution of traps should be somewhat exponential with a density in the range of 10^{-5} - 10^{20} per cubic centimeter.[3]

Various techniques have been employed in the investigation of radiation induced

space charge build-up in solid dielectrics. Solid dielectrics have been irradiated and then a sharp grounded probe applied to the surface to initiate charge release.[4] Photographic records of charge build-up in Lucite have been obtained.[5] In Reference 5 it is particularly interesting to note the apparent reduction in the electron range in the Lucite as a retarding electric field builds up in the block. Dielectrics have been electron irradiated and then given a heat treatment to induce discharge.[6] Experimental investigation of capacitor type structures have also been performed.

In much of the preceding work on space charge build-up in solid dielectrics either the dielectric was of a sufficient thickness to completely stop the incident electrons or the electron energy was adjusted so that electrons would be completely absorbed within the available dielectric thickness. In either case the amount of deposited charge was maximized. It has been determined that the maximum charge is deposited within the dielectric if the range of the incident electron is approximately one-half the dielectric thickness.

Our test series, of course, utilizes an aluminum mylar, copper structure (Figure 16) exposed to a 90 Sr source whose Beta spectrum is shown in Figure 17.

The electrons are incident on the aluminum electrode of the capacitor panel (Pegasus Micrometeorite Detector Panel). Only those pulses arising from the spontaneous decay of charges trapped in the dielectric of the capacitor nearest to the electron source were recorded. Using Beta particle range theory the energy loss of the primary electrons as they travel through the capacitor can be calculated.

For $0.01 \leq E \leq 2.5$ MeV

$$R = 412\, E^{1.265 - 0.0954 \ln E}$$

$$\ln E = 6.63 - 3.2376 \left[10.2146 - \ln R\right]^{1/2}$$

Where R = Range in mg/cm^2

E = Maximum energy, MeV.

However, a knowledge of the energy deposition due to primary electrons alone is not sufficient. When electrons travel through a medium they loose energy by excitation, ionization, and bremsstrahlung. These processes may and do contribute secondary electrons to be considered in the overall charge deposition scheme. The bremsstrahlung or x-rays will be attenuated through the production of Compton and photoelectrons.

A thorough consideration of the electron flux incident on the capacitor yields the following rather complicated picture of the capacitor panel in an environment of energetic electrons and x-rays.

(1) Electrons with energy $\leq$ approximately 426 keV are stopped in the 0.4 mm Al electrode (for 0.2 mm electrode, $E \leq$ 240 keV and for 0.04 mm Al electrode, $E \leq$ 162 keV).

(2) Primary electrons with $E >$ 427 keV plus secondary electrons (Compton electrons, photo-electrons, recoil electrons) plus x-rays enter the mylar.

(3) Electrons with energy $\leq$ approximately 19 keV are stopped in the mylar. X-rays are attenuated in the mylar. Traps in addition to those initially present are created. Some traps are filled.

(4) Electrons and x-rays are backscattered from the copper electrode and other surrounding materials into the mylar.

(5) Electrons with energy $\leq$ approximately 20 keV are stopped in the copper electrode.

(6) Primary electrons penetrate the entire panel and backscatter into the copper electrode where x-rays and secondary electrons again are created and

scattered toward the mylar.

Based on the preceding breakdown it would not be unreasonable to assume either a uniform trapped charge density throughout the dielectric or a trapped charge density that would be greater near the two electrodes than at the center of the dielectric. It could be assumed that the effect of the primary electrons, most of which are sufficiently energetic to penetrate the entire dielectric, plus the profusion of secondary radiations could result in a homogeneous charge distribution. It could also be argued that the range of the secondary radiations is not sufficient to penetrate through the entire dielectric and since the secondary radiations originate on each side of the dielectric that a greater space charge would build up near each electrode. Further experimentation to define the characteristics of the secondary radiations is required before any definitive conclusion can be reached.

The physical thickness of the mylar dielectric is 0.6 mg/cm^2 using beta particle range theory this thickness is equivalent to the range of a 19 keV electron. However, since a large retarding electric field does build up then the effective thickness of the dielectric may be much greater. This would result in the deposition of a larger charge than predicted by the conventional theory.

Experimental evidence collected indicates that the mechanism of trapped electron discharge may be considered as a two stage process. The simplest model assumes that electrons are trapped within the dielectric and a uniformly distributed space charge builds up. This uniform charge will build up to some level at which the associated electric field will exceed the breakdown strength of the dielectric and a discharge to one of the capacitor electrodes will occur. The maximum discharge pulse observed was on the order of two volts. This indicates that the entire dielectric did not release it's charge but that indeed a localized small area breakdown occurred. An essentially complete spectrum of discharge pulse amplitudes up to the maximum amplitude was observed. For localized breakdown the amount of charge liberated is probably confined

to the region near a defect since the intrinsic characteristics of the dielectric will only be affected in a finite region around the defect. Repetitive pulsing in which as many as three pulses occurred in less than 10 milliseconds was observed. This further substantiates the small area breakdown theory since the maximum primary electron flux is approximately 5×10^8 e/cm^2/sec and sufficient recharge time had not elapsed. The first stage of the discharge process is then considered to be a release of trapped charge to the capacitor electrode. The discharge occurs in finite time and it is assumed that the time required is a characteristic of the mechanism which caused the discharge. The second stage of the process then is simply a return to equilibrium by capacitor discharge through the load resistor with the characteristic RC time constant. Variation of the load up to 10 k ohms affected the discharge time only.

The aluminum electrode of the capacitor was connected to the pulse recording electronics and the copper electrode grounded. With this configuration the number of negative pulses observed was greater than the number of positive pulses. However, the pulse rate was rather low and this observation may be a problem of statistics. If this observation were correct then a non-uniform space charge distribution could be postulated. In the case of the metal-insulator-metal capacitor structure where dissimilar metal electrodes are used the shape of the potential barrier will be trapezoidal. Significant changes in the barrier could be caused by the addition of trapped charges near the electrodes.[9] This could possibly have an effect on the positive to negative pulse ratio.

A temperature effect on pulse rate was also observed as an increase in pulse rate with decreasing temperature down to the minimum -62°C attained in this test. This may be attributed to the electrical conductivity "J" which has the temperature dependence predicted by

$$= Ae^{-E/RT}$$

where E is the activation energy. The temperature effect could also be associated with the deactivation of trapping sites as the temperature is reduced.

The effects of polarization of the dielectric by an applied field have not been considered in this effort. No bias was applied therefore no net internal polarization should be present.

The study of space charge buildup and spontaneous discharge in mylar capacitor structures should be carried forward as a fundamental research project aimed at a characterization of the various contributing phenomena.

4.0 PEGASUS ELECTRONICS AND PANEL EXPERIMENTS

The Pegasus electronics was connected to the micrometeorite panels for all of the following tests. A 16 mil panel was used and in difference to the prior tests, the copper side of the panel was connected to the center conductor of the coax and the shield was to the aluminum. All data was taken with the panel in a biased condition.

4.1 HARDWARE ARRANGEMENT

To facilitate the measurement requirements a number of modifications to the test system were made. Figure 8 depicts the Pegasus panel mounting used in the environmental chamber.

In an effort to reduce the panel temperature variations when the radiation shield was removed an accordion type folding screen was employed. This screen collapses to the bottom of the inner chamber to expose the Pegasus panel to the radiation source. A finned radiator was added between the shutter and Pegasus panel to improve the panel to chamber temperature response time.

The environmental temperature control sensing thermocouple was attached directly to the Pegasus panel to ensure proper temperature settings. (The system is normally controlled by the circulating brine temperature which responds faster than a test item within the chamber).

An automatic temperature and radiation cycle control unit was constructed to enable tests to be run continually. "Hit" monitoring circuitry was changed as shown in Figure 9.

4.1.1 Pre-Test Hardware Evaluation

In setting up and adjusting the equipment a number of interesting hardware characteristics were noted and taken into consideration when evaluating the data.

There are three "hit" threshold levels within the system. These levels are dependent upon panel discharge wave shape and can only be approximated as to their amplitude. The first is the level which can be detected by the pulse inverter and subsequently recorded. This lies at about 0.3 V. The second is the point at which the Pegasus electronics will produce a "pulse verify" output without any signal lights illuminated. This threshold is about 1.0 V. The third level of about 1.2 volts will produce a signal light indication and a pulse verify.

The panel seemed extremely sensitive to electromagnetic interference. A fractional horsepower squirrel cage induction motor mounted outside the temperature controlled housing but within the vacuum chamber (See Figure 8) will, when energized, cause the panel to discharge sufficiently to produce both a pulse verify and signal light condition.

To maintain temperature within the chamber the environmental control system cycles a valve in the refrigeration compressor. This valve is outside the vacuum chamber and about fifteen feet away. Cycling of this valve causes the panel to discharge at an amplitude sufficient to be recorded. This discharge is not detected by the Pegasus electronics.

4.2 DISCUSSION OF PANEL PLUS ELECTRONICS EXPERIMENTS

In the following section each test is described and discussed separately.

4.2.1 Temperature Versus Pulse Rate

The panel temperature was varied in 10°C steps from 0°C to -60°C. At each of the temperatures 0, -10, -20, -30, -40, -50, and -60°C, the breakdown pulse rate was determined with ample time being allowed at each step to assure that charge equilibrium had been reached.

Figure 10 displays the relationship between the total number of pulses recorded and the verified pulses over the required temperature range. Although the two curves are not similar in shape they do verify earlier conclusions that under a constant radiation environment the pulse rate tends to increase with a decrease in temperature with the majority of the pulses being low level.

4.2.2 Spectrum - Temperature

Six pulse height spectrums were obtained under the following conditions.

a. The panel was irradiated for at least 8 hours at -40°C. The radiation shield was then closed and the panel heated at maximum rate until its temperature reached +40°C. During this heating cycle a pulse height spectrum was obtained.
b. same as a except heated to +20°C.
c. same as a except heated to 0°C.
d. same as a except started at -20°C and heated to +40°C.
e. same as d except heated to +20°C.
f. same as d except heated to 0°C.

Before each of the six temperature cycles run for spectral analyses the panel was allowed to stabilize at the lowest temperature of the cycle for sixteen hours.

Figure 11 is a graphical representation of the data obtained. Each chart shows the temperature change versus time, the number of pulses recorded during ten minute intervals, and the total number of pulses verified by the Pegasus electronics.

The pattern of each run is about the same regardless of starting point with the pulse rate increasing with an increase in temperature. The significant factor appears to be the total time of the temperature cycle as depicted by the -40°C to +40°C chart. There was, apparently, sufficient time for the panel to substantially discharge itself.

Figure 12 shows the pulse amplitude spectrum for each run. Of importance is the fact that no pulses appear at the one volt threshold level. As was stated before the electronics package appears to be wave shape sensitive and accepted some of the lower amplitude pulses as verified hits. The largest spectral response is in the low level pulses below the recorder threshold.

4.2.3 Radiation Cycling

The panel temperature was lowered to -60°C and a 90 minute off - 10 minute on radiation cycling programmed. This test condition was then maintained for 64 hours. Numerous low level hits were recorded. The only verified pulses observed were those corresponding to shutter cycling transients. This run indicates that at a constant low temperature there is no increase in panel discharges as a result of short time exposure to a high level radioactive environment.

4.2.4 Radiation and Temperature Cycling

The panel temperature was stabilized at -60°C and then heated at maximum rate to +40°C whereupon recooling commenced to return the panel to -60°C. During this temperature excursion the radiation was cycled on a 10 minute on, 90 minute off basis. "Hits" were recorded continuously. This run proved to be a verification of

those preceding it. The temperature and radiation were cycled automatically and continuously for a two week period. As before the most significant change was due to temperature and manifested itself as an abrupt increase in pulse production as the temperature started to increase with a gradual tapering off as the panel lost its charge (Figure 13). As the panel temperature was lowered the number of low level pulses started to increase (Figure 14). There were several "hits" verified by the electronics package each day but these were random in nature with none occurring during an irradiation period.

One exception to the case is shown in Figure 15. In this run, which took place during the night, a momentary power failure dropped out the refrigeration system which allowed the panel temperature to increase slowly while the radiation continued cycling. The discharge rate still followed about the same curve with an increase and then a gradual tail off but interestingly there was a discernable increase in rate during the irradiation periods. This was not repeated in any of the other runs nor were there any unusual verified hits.

REFERENCES

1. Theoretical Analysis of Operational Characteristics of Micrometeoroid Capacitor Detector, Prepared under Contract NAS1-3343 by the Solid State Laboratory of the Research Triangle Institute, Durham, North Carolina.

2. L. K. Monteith, Trapping and Thermal Release of Irradiation Electrons from Polyethylene Terephtholate Films, J. Appl. Phys. 37, 1966, pp 2633-2637.

3. A. Charlesby, Atomic Radiation and Polymers, Pergamon Press, 1960.

4. J. Furuta, E. Hiraoka, and S. Okamoto, Discharge Figures in Dielectrics by Electron Irradiation, J. Appl. Phys. 37, 1966, pp 1873-1878.

5. H. Lackner, I. Kohlberg, and S. V. Nablo, Production of Large Electric Fields in Dielectrics by Electron Injection, J. Appl. Phys. 36, 1965, pp 2064-2065.

6. P. V. Murphy and S. C. Ribeiro, Polarization of Dielectrics by Nuclear Radiation. I. Release of Space Charge in Electron Irradiated Dielectrics, J. Appl. Phys. 34, 1963, pp 2061-2063.

7. Y. Invishi and D. A. Powers, Electric Breakdown and Conduction through Mylar Films, J. Appl. Phys. 28, 1957, pp. 1017-1022.

8. B. Gross, Beta Particle Transmission Currents in Solid Dielectrics, J. Appl. Phys. 31, 1960, pp 1035-1037.

9. D. V. Geppert, Theoretical Shape of Metal-Insulator-Metal Potential Barriers, J. Appl. Phys. 34, 1963, pp 490-493.

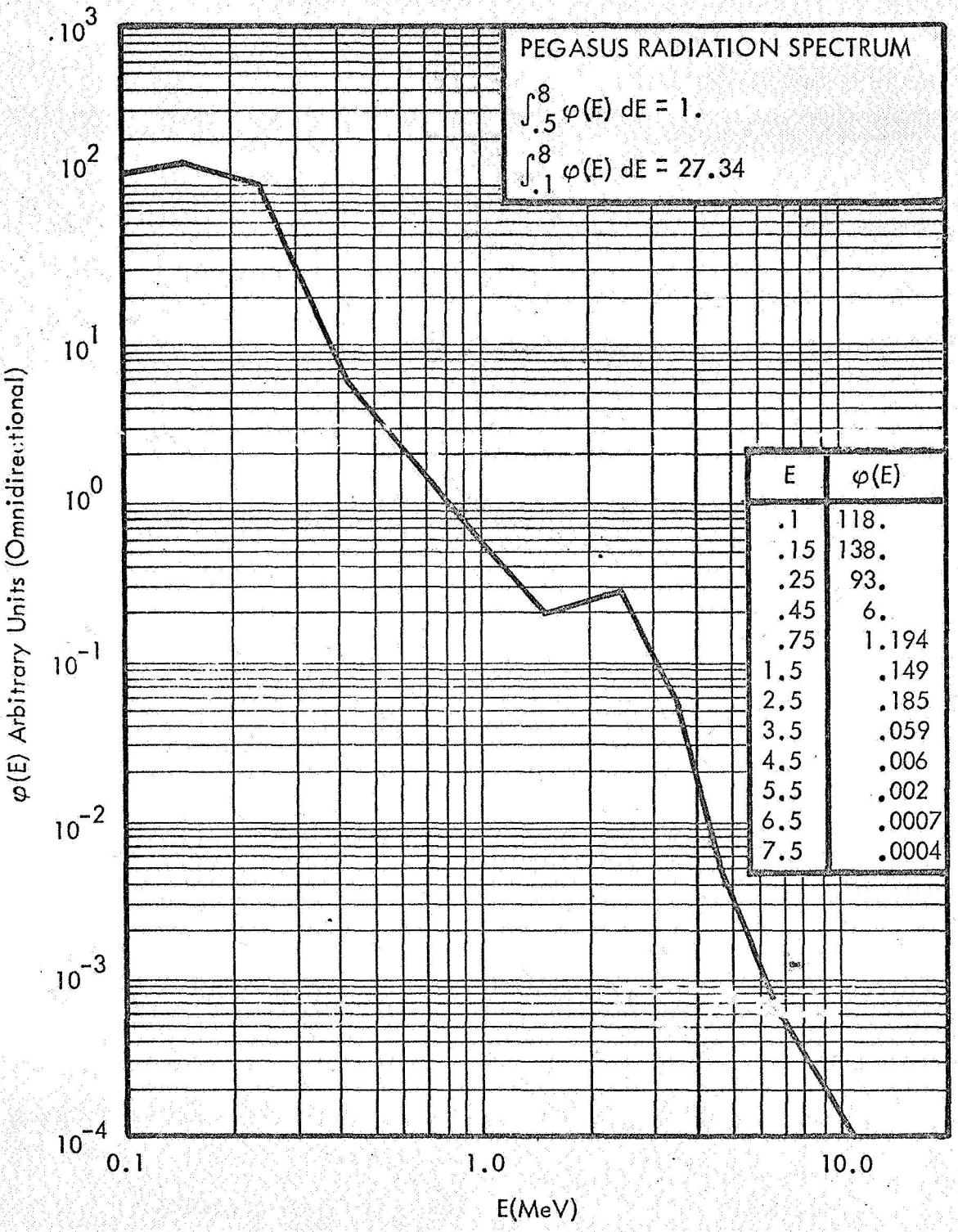

FIGURE 1 APPROXIMATE PEGASUS SPACE ELECTRON SPECTRUM

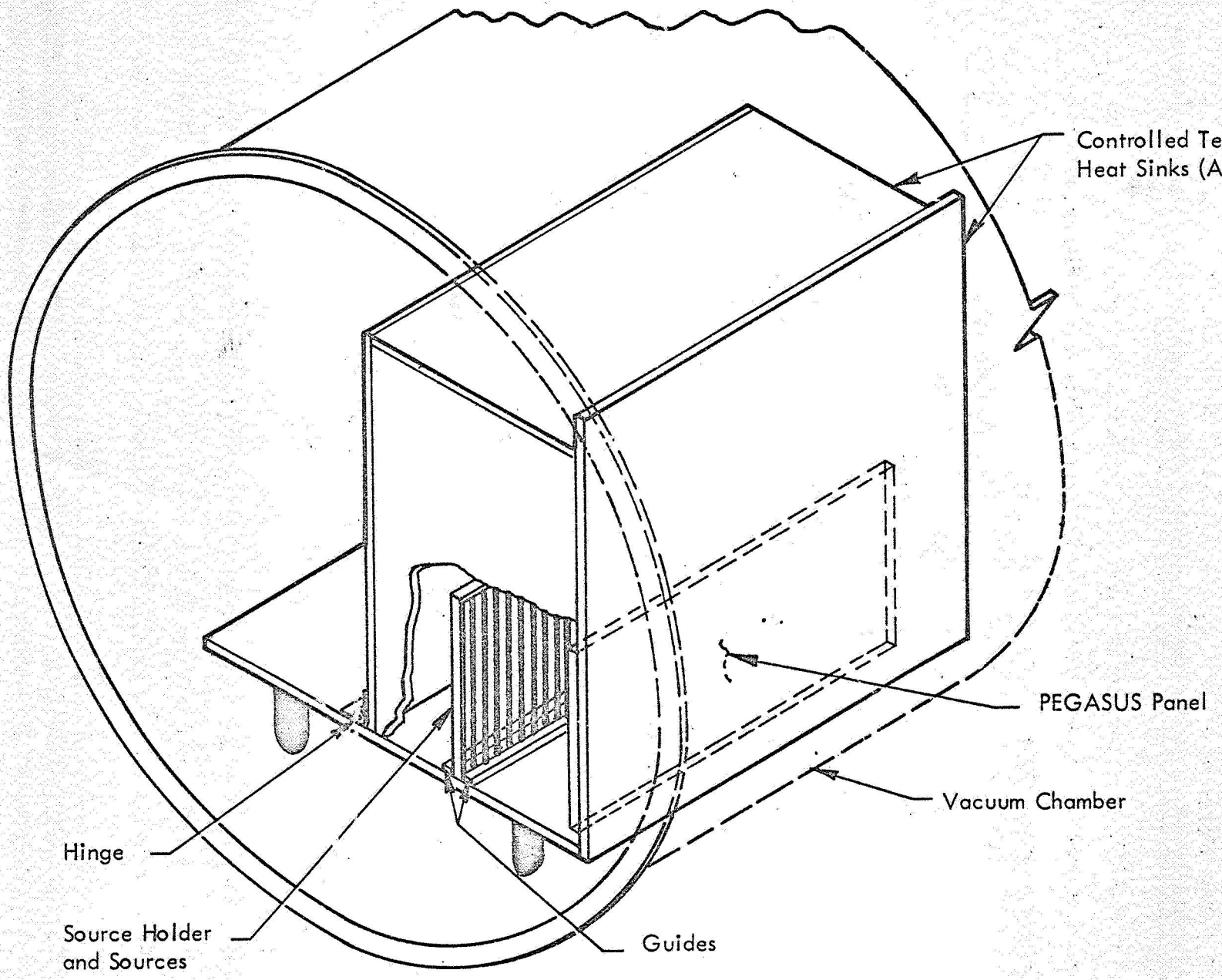

FIGURE 2 SOURCE AND PEGASUS PANEL IN THE HEAT SINK

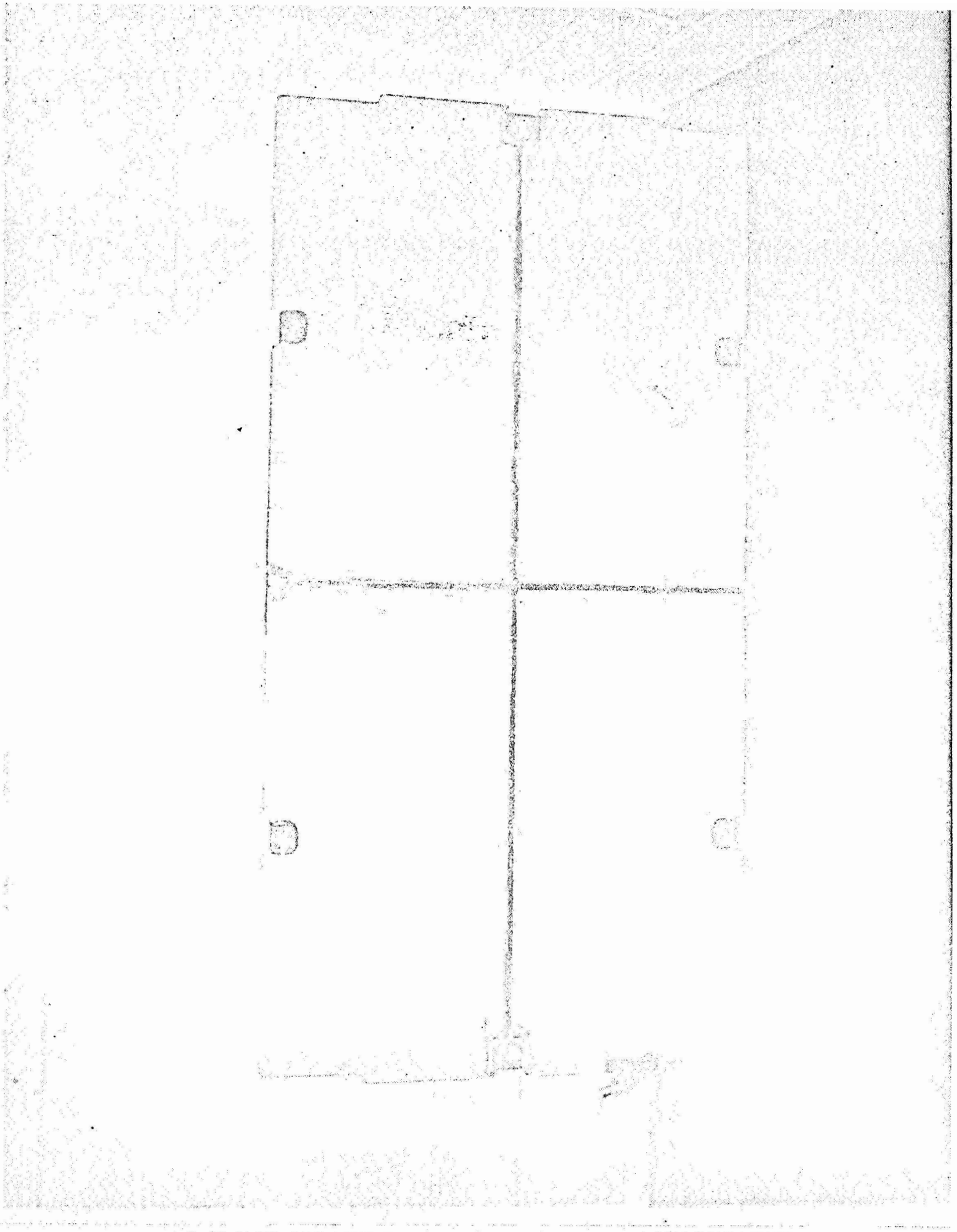

FIGURE 3 ETCHED PEGASUS PANEL FOR SMALL AREA BREAKDOWN TEST

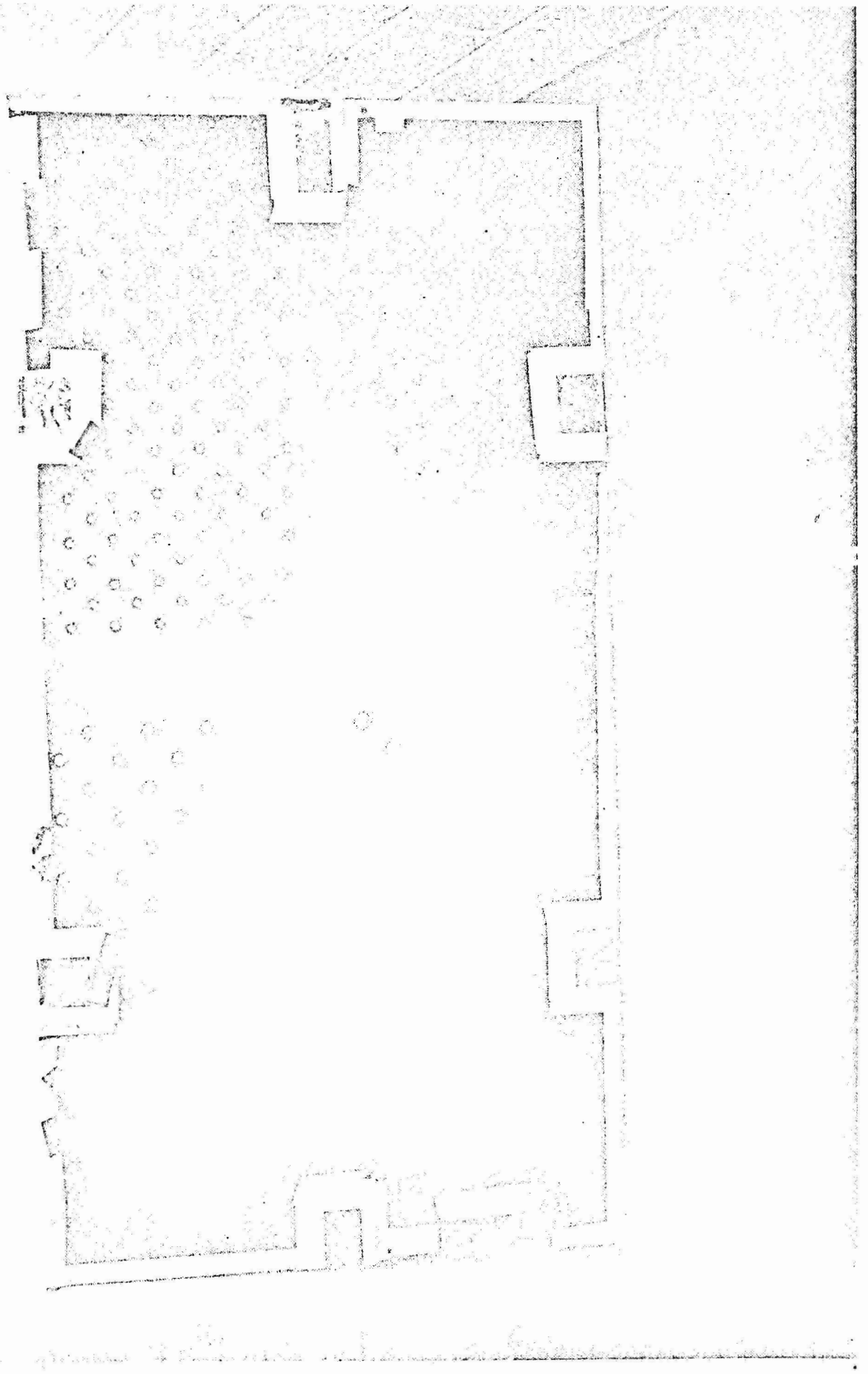

FIGURE 4 PEGASUS PANEL SHIELD SMALL AREA BREAKDOWN TEST

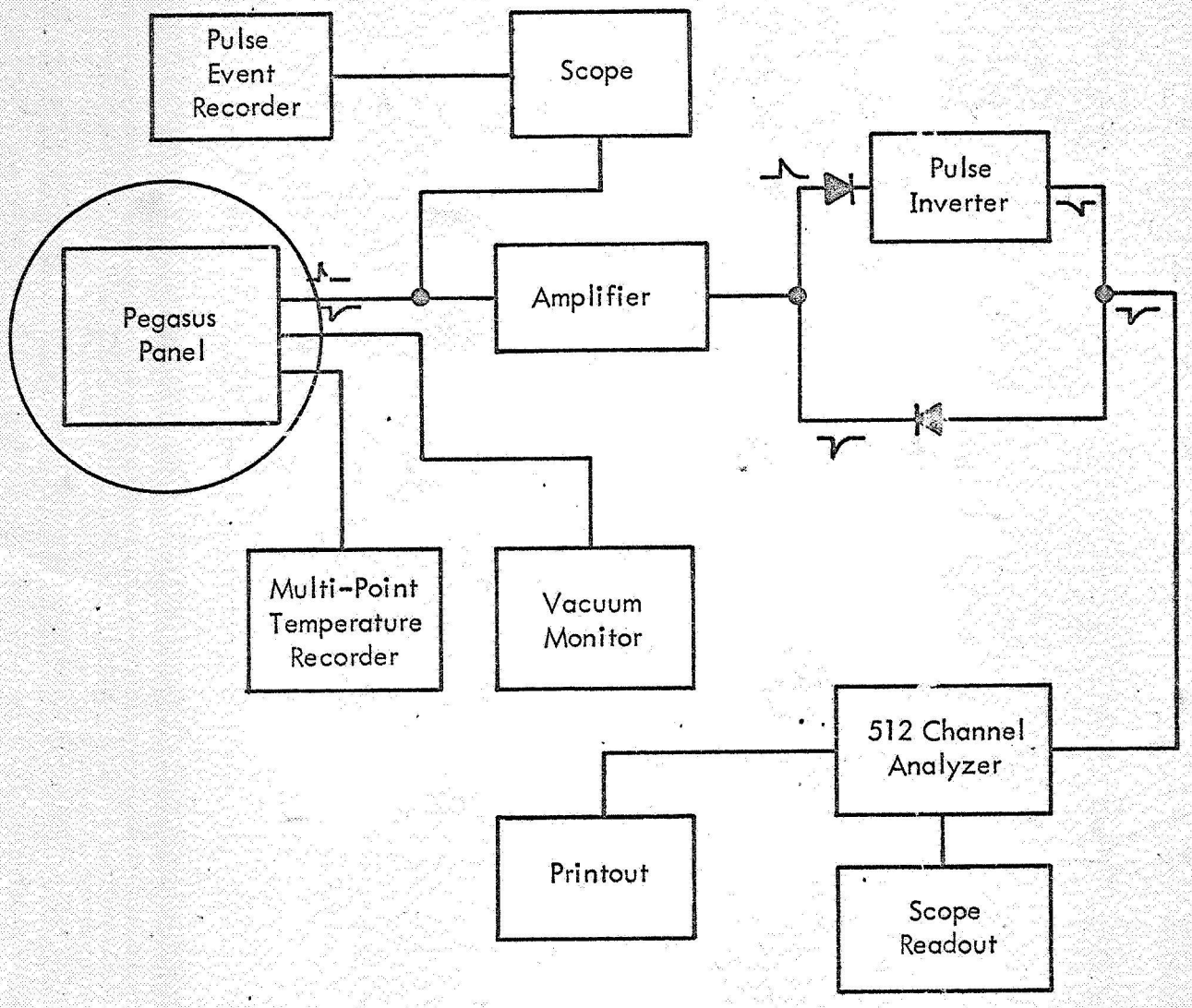

FIGURE 5 BLOCK DIAGRAM - TYPICAL PANEL INSTRUMENTATION SYSTEM

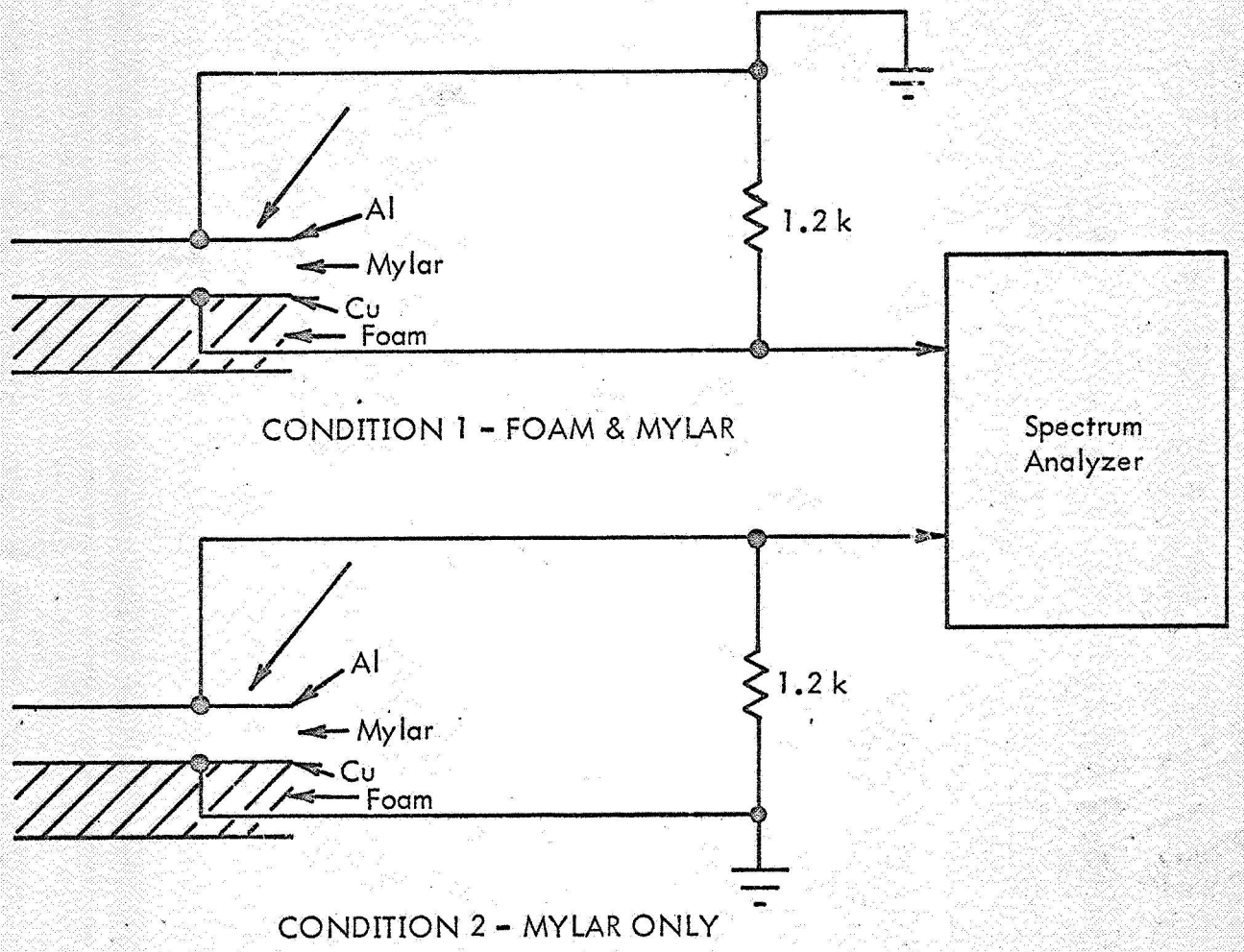

FIGURE 6 MONITORING CIRCUITS FOAM EFFECT

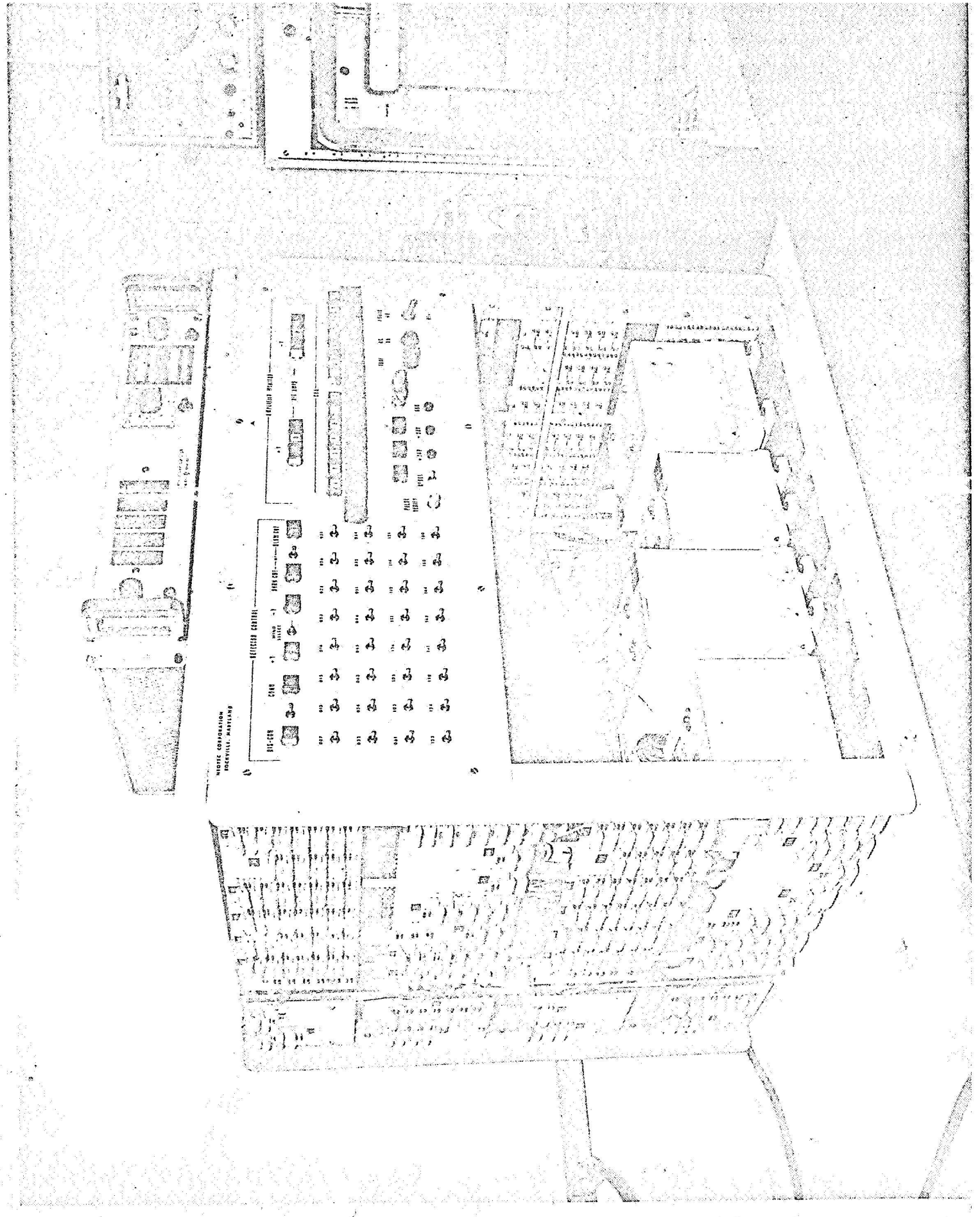

FIGURE 7 PEGASUS MICROMETEOROID DETECTION SYSTEM

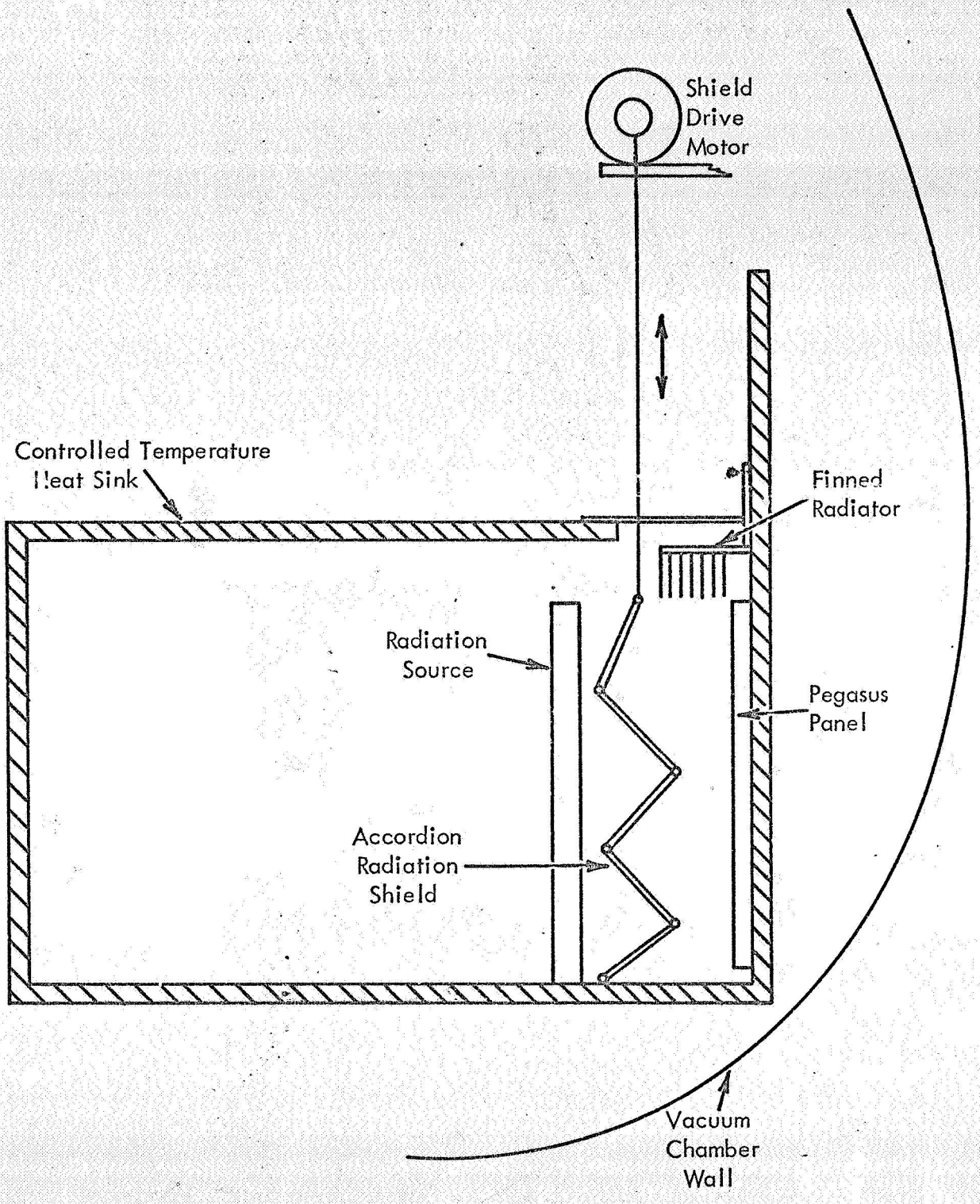

FIGURE 8 VACUUM CHAMBER LAYOUT

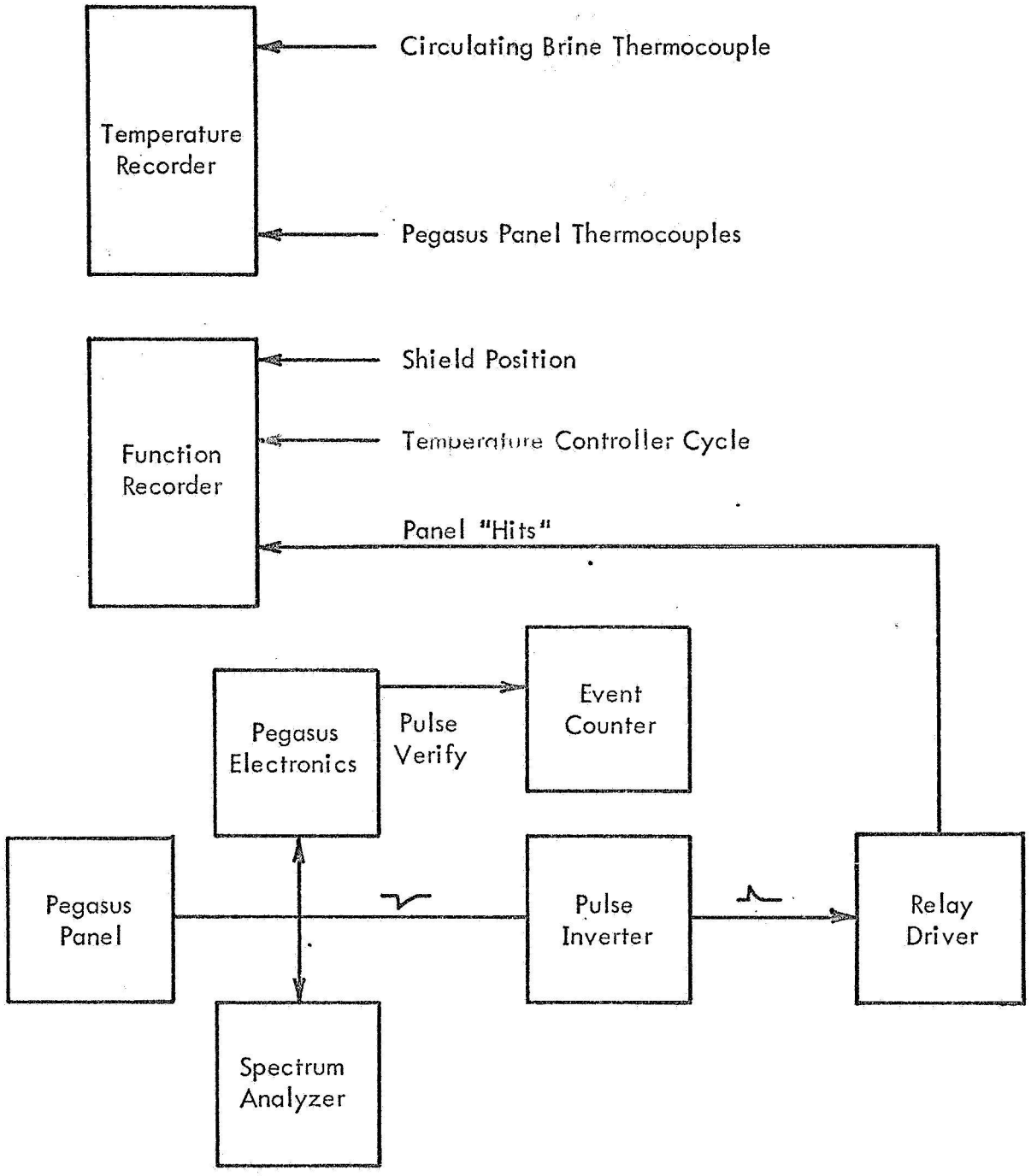

FIGURE 9 MONITORING CIRCUITS

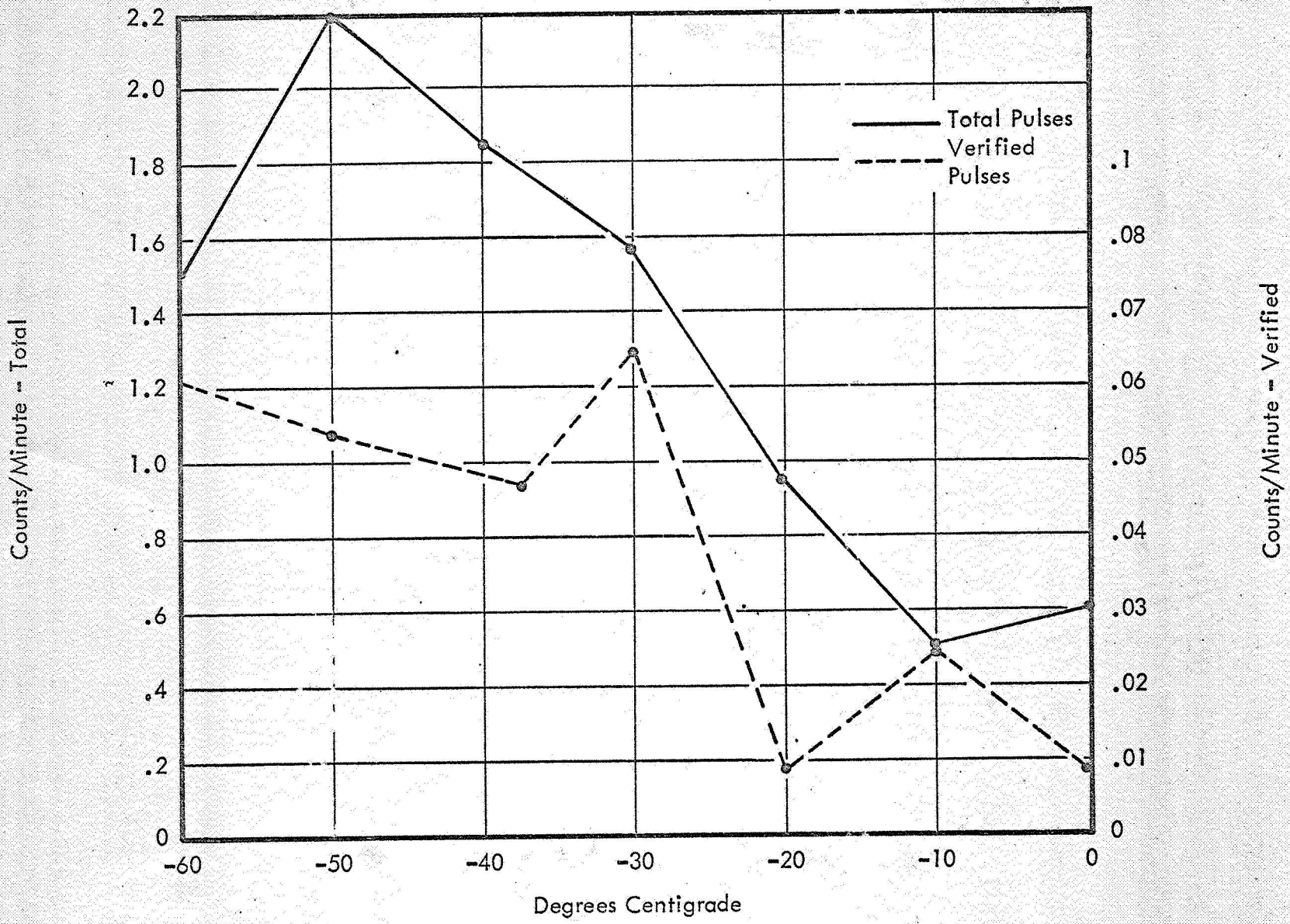

FIGURE 10 TEMPERATURE VERSUS PULSE RATE

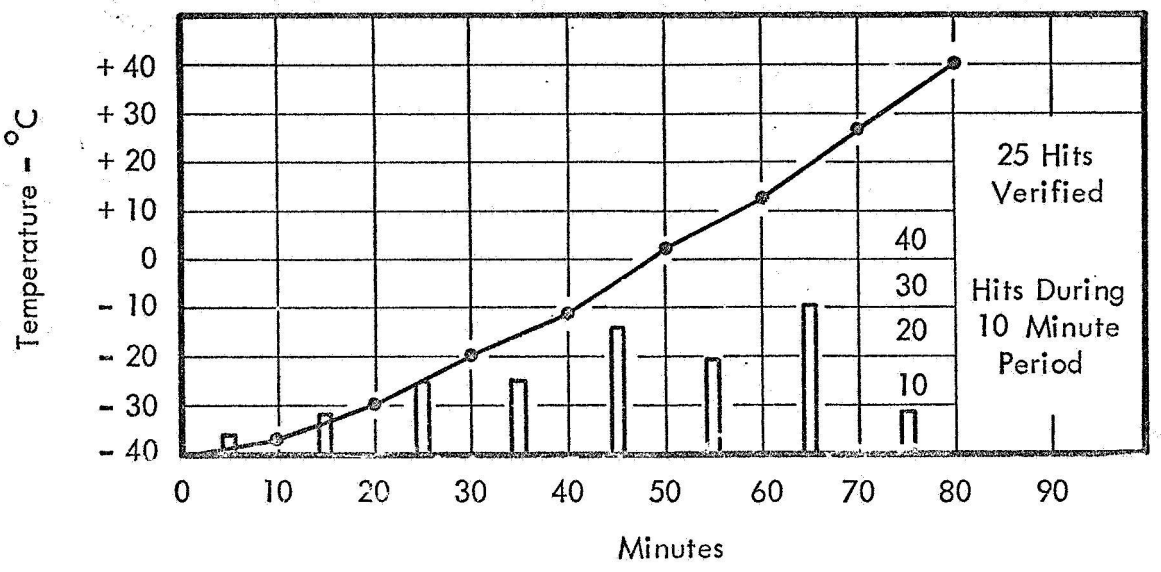

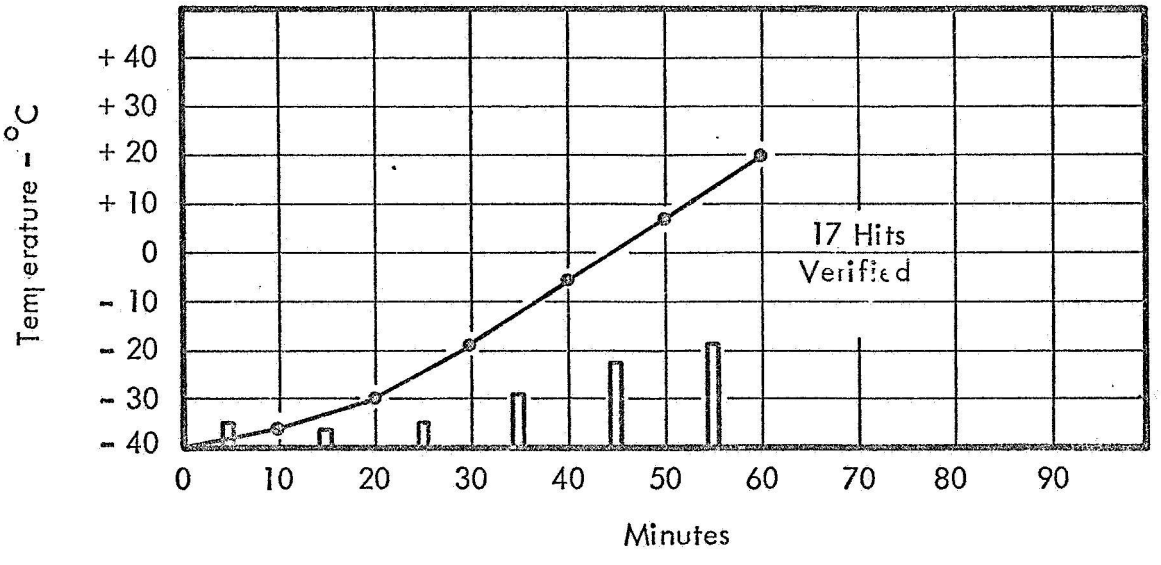

FIGURE 11A VERIFIED HITS VERSUS TEMPERATURE

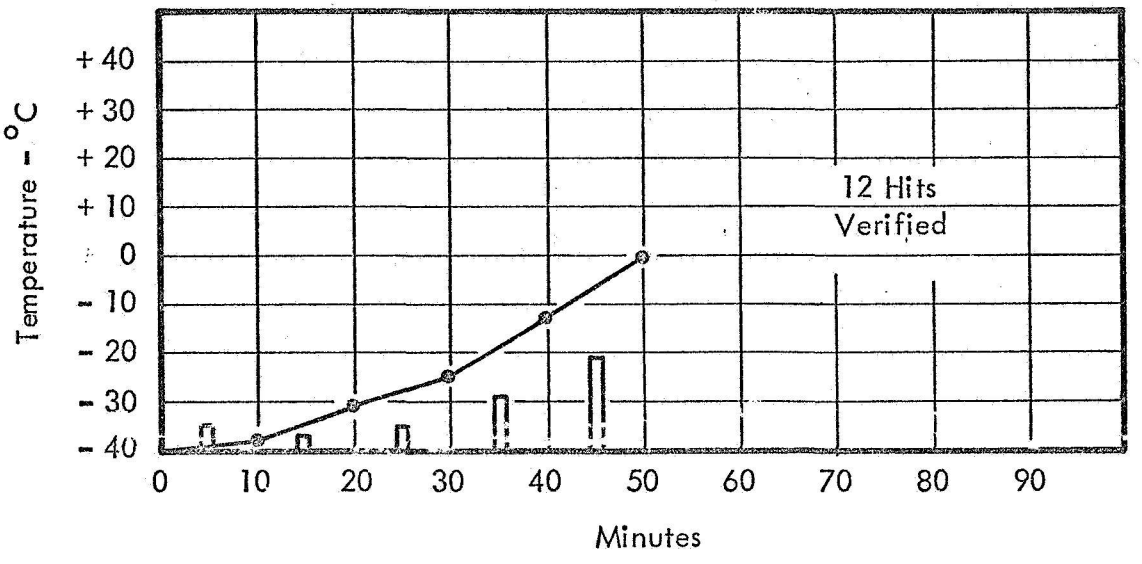

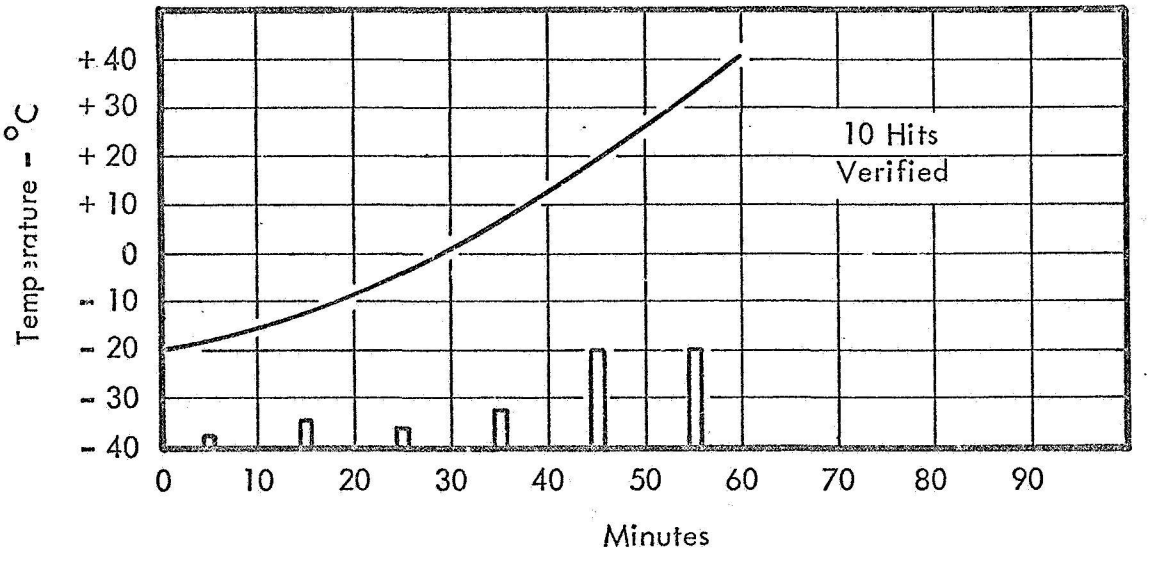

FIGURE 11B VERIFIED HITS VERSUS TEMPERATURE

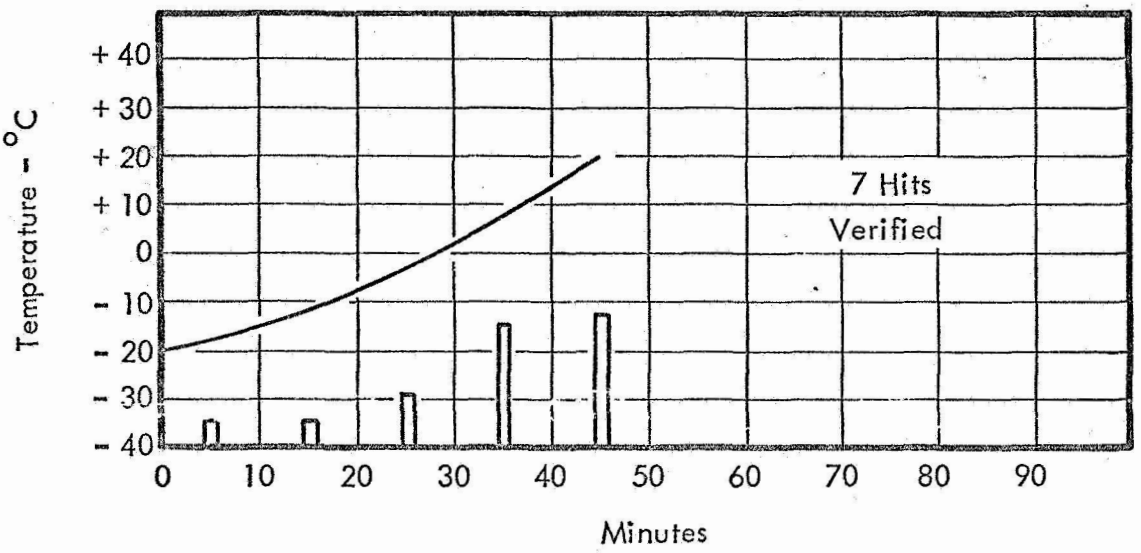

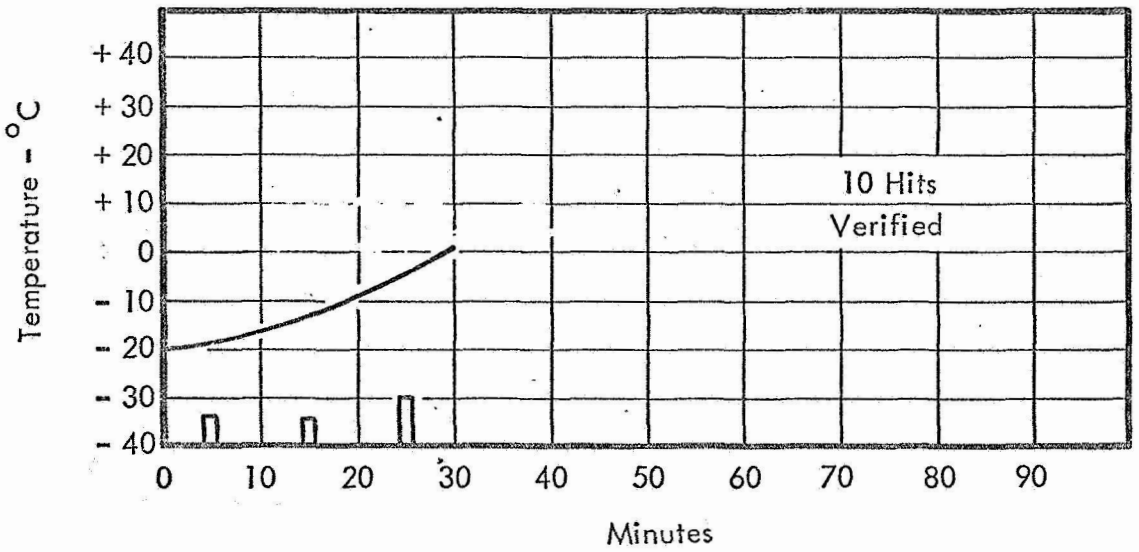

FIGURE 11C VERIFIED HITS VERSUS TEMPERATURE

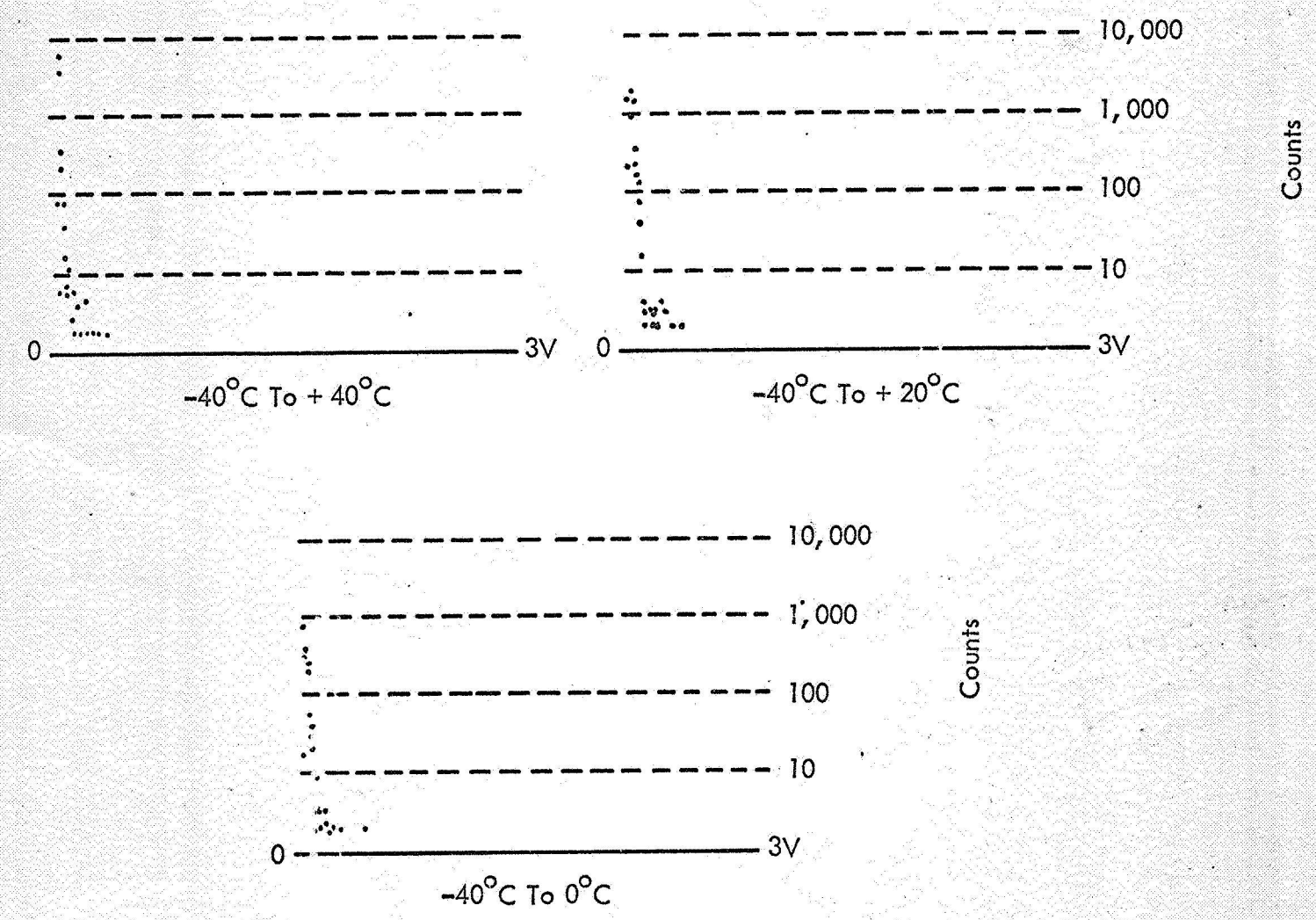

FIGURE 12A SPECTRUM VERSUS TEMPERATURE

FIGURE 12B SPECTRUM VERSUS TEMPERATURE

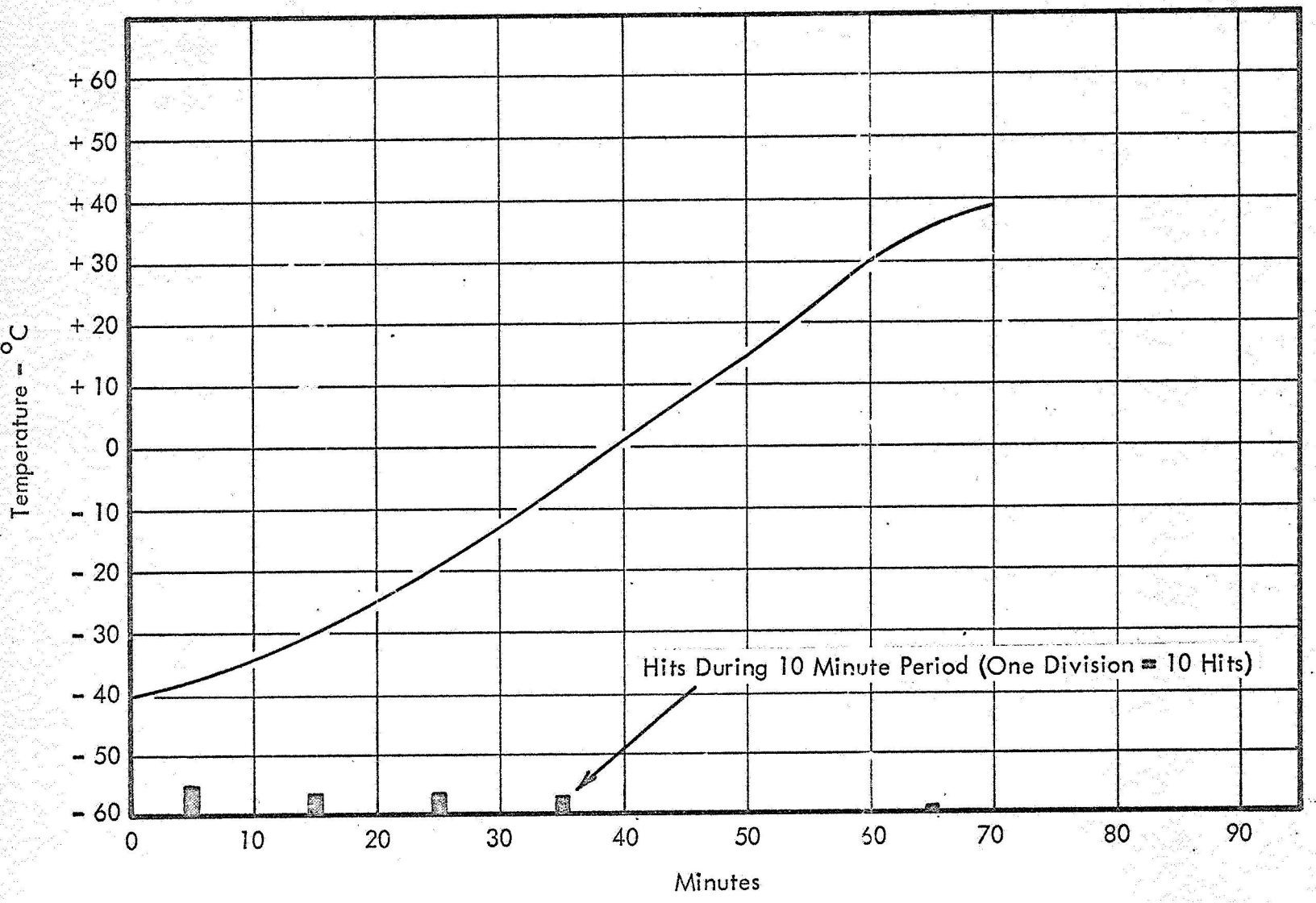

FIGURE 13A RADIATION AND TEMPERATURE CYCLING

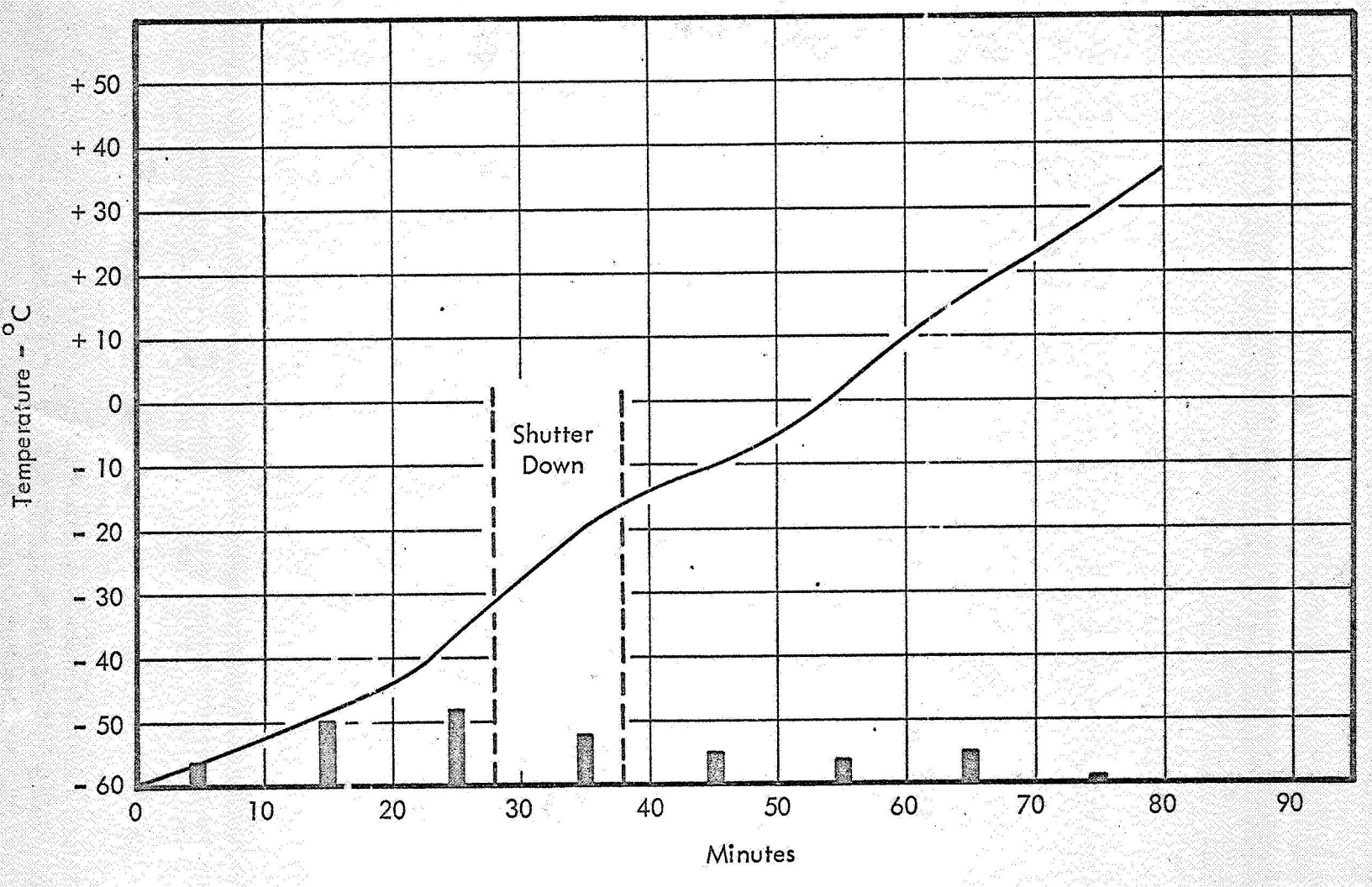

FIGURE 13B RADIATION AND TEMPERATURE CYCLING

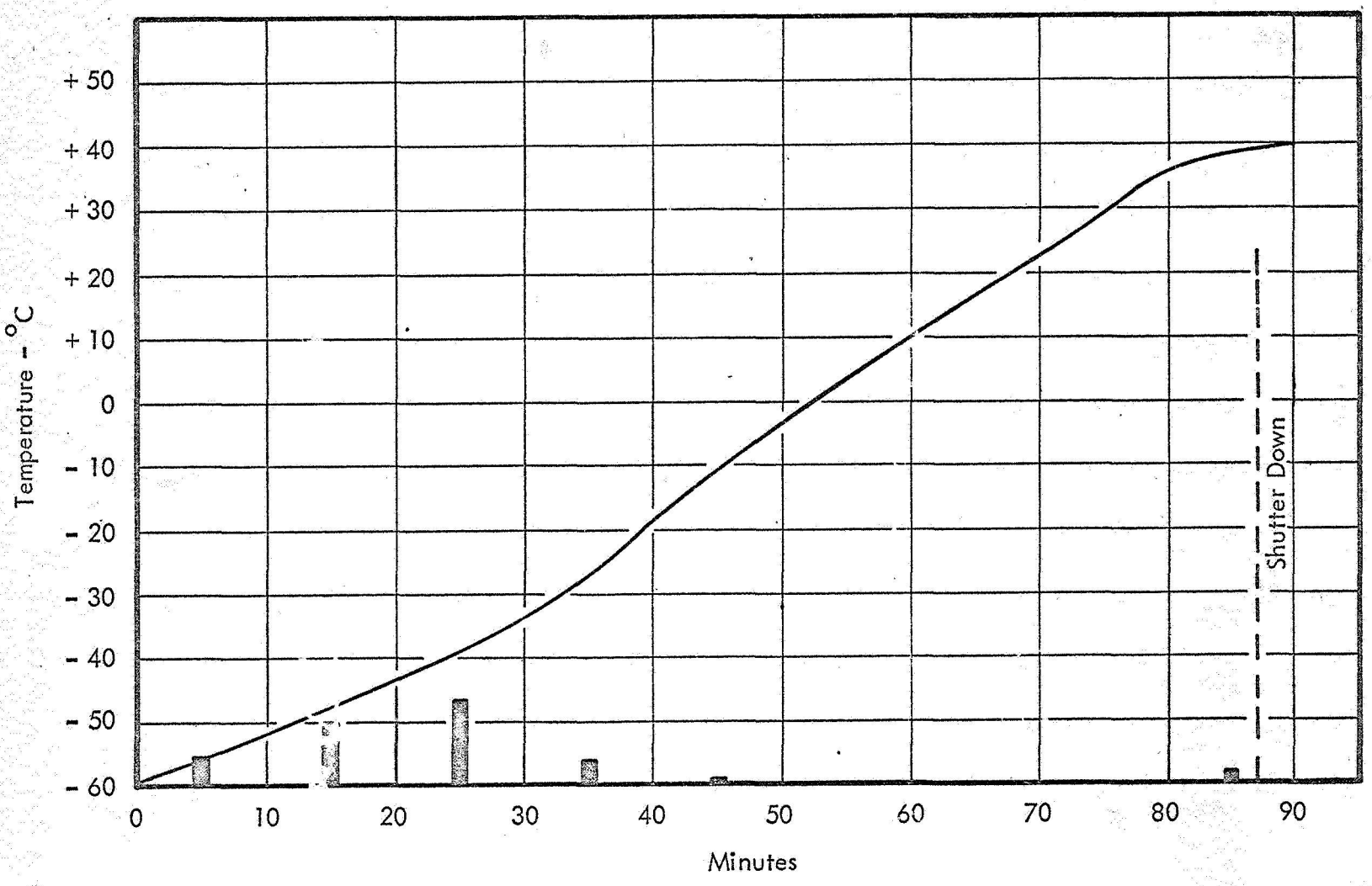

FIGURE 13C RADIATION AND TEMPERATURE CYCLING

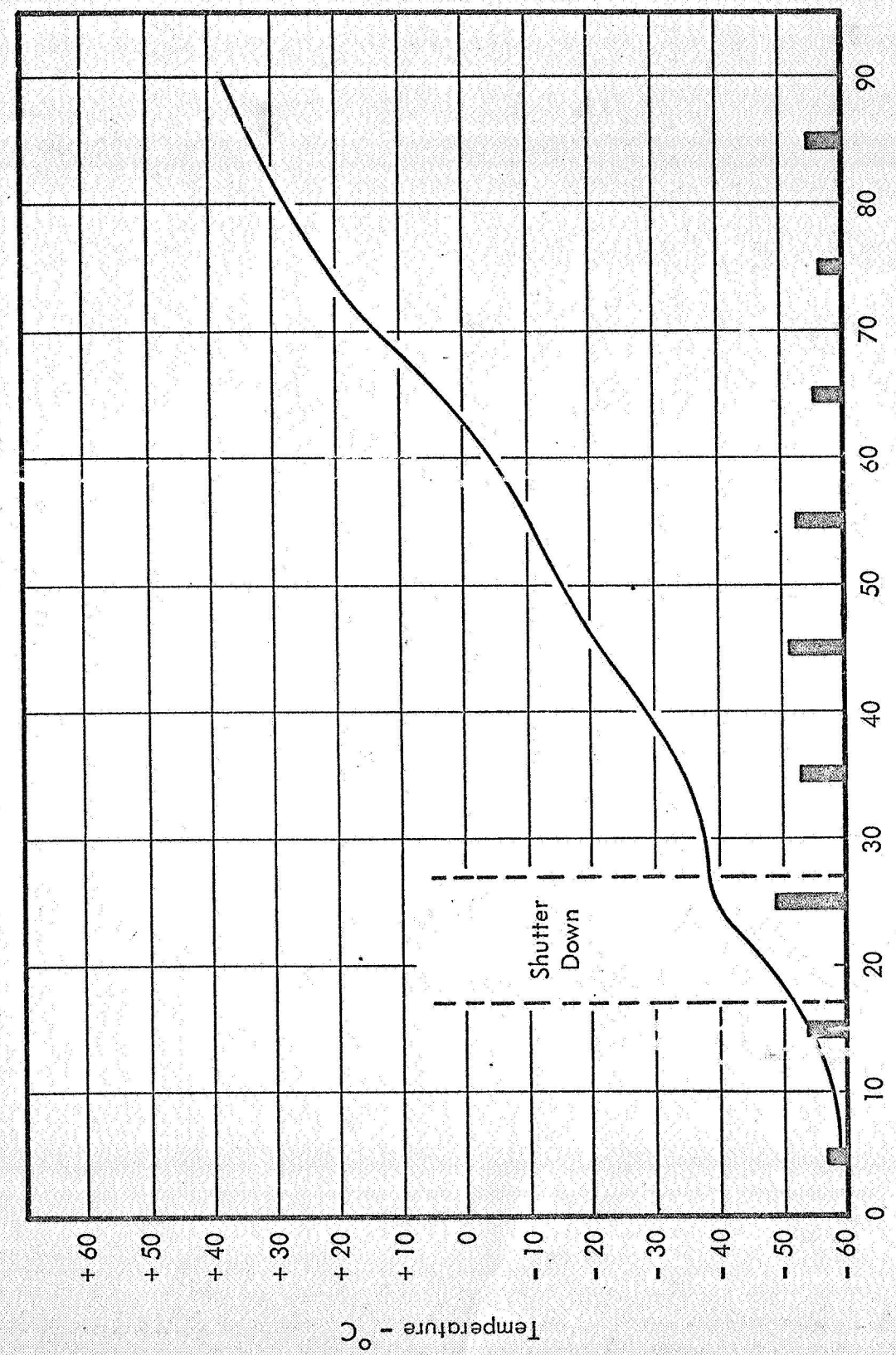

FIGURE 13D RADIATION AND TEMPERATURE CYCLING

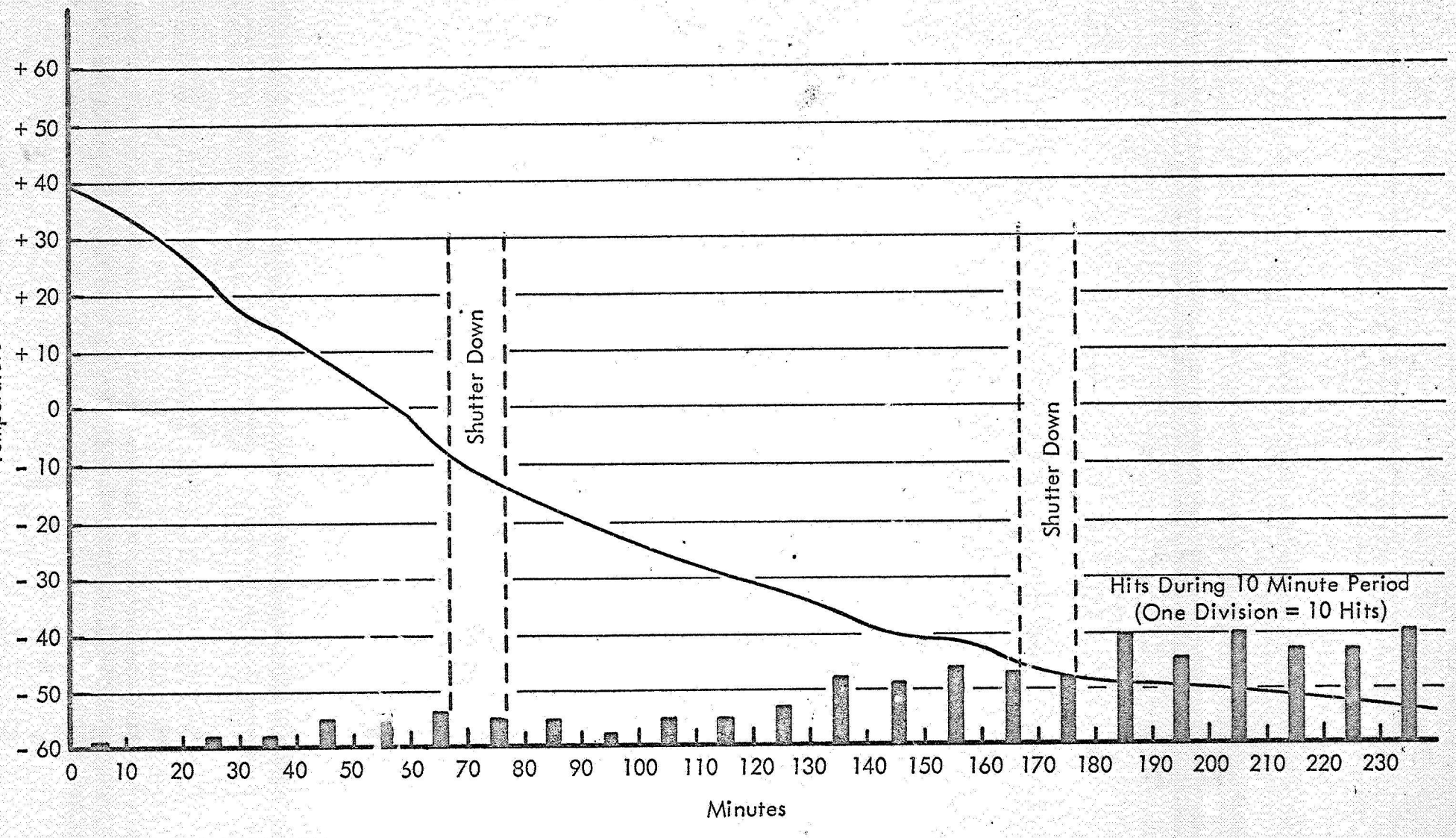

FIGURE 14A RADIATION AND TEMPERATURE CYCLING

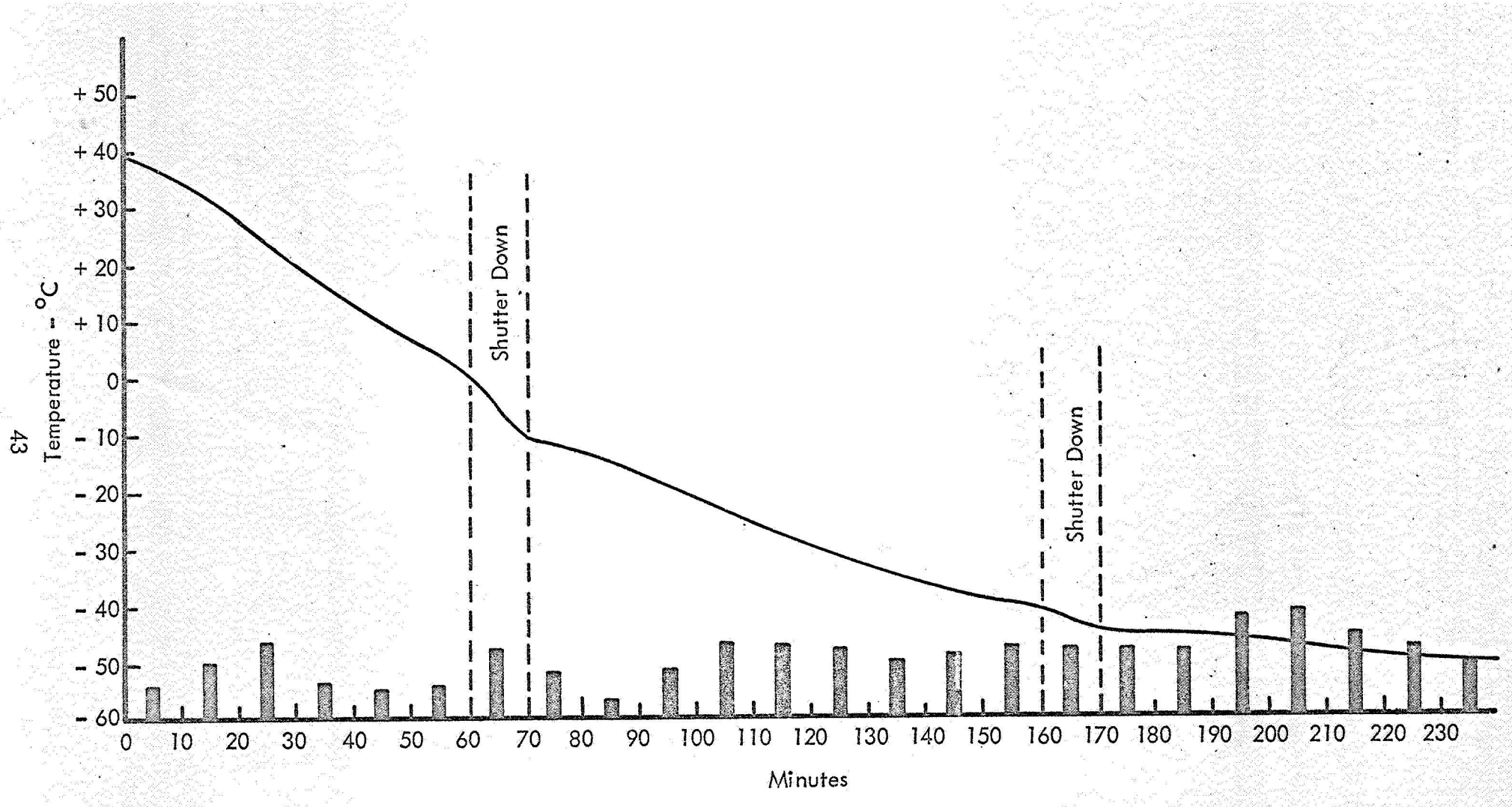

FIGURE 14B RADIATION AND TEMPERATURE CYCLING

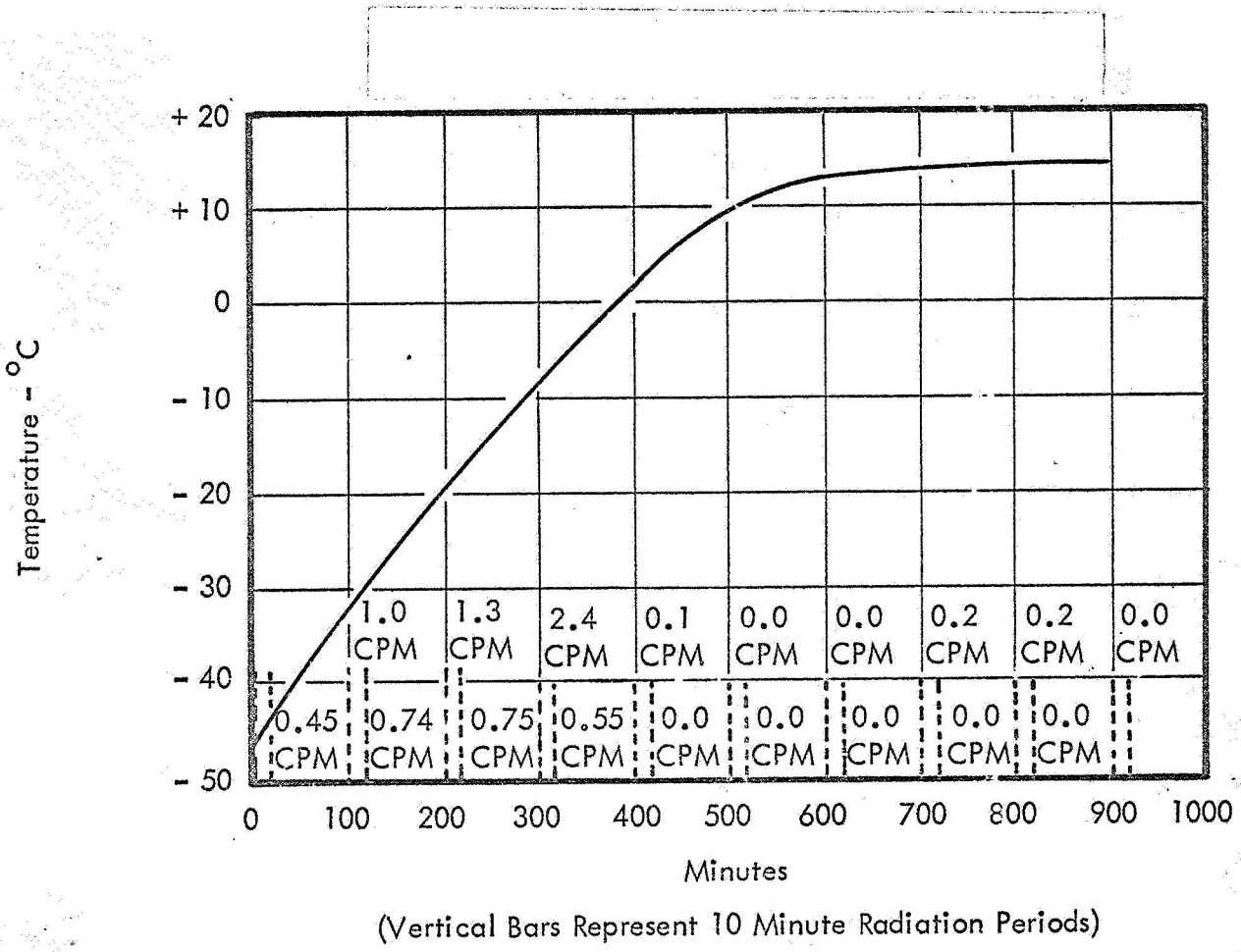

FIGURE 15 SPECTRUM WHEN MOMENTARY POWER LOSS DROPPED OUT COOLING SYSTEM AND PANEL GRADUALLY WARMED UP